

Supplemental Methods and Materials

Cell culture

Jurkat cell stocks (ATCC) (5×10^6) were thawed from cells stored in liquid nitrogen (LN2). Cells were cultured at 37°C, 5% CO₂ for one week in RPMI media, containing 10% FBS, 2mM Glutamine, 100 U/ml Penicillin, and 100 µg/ml Streptomycin. Twenty-four hours prior to an experiment cells were washed and serum starved for 16 hours by culturing in RPMI in bacterial plates to prevent adhesion. After 16 hours, cells were synchronized by culturing in 50% FBS for two hours, washed twice with RPMI, followed by 6 hours of culture in serum free RPMI. To start the experiment, cells were concurrently treated with the following reagents as described in the figures: 0.5 µg/ml CD3, 0.5 µg/ml CD28 (Miltenyi #s 130-093-387, 130-093-375), and 1 nM prostaglandin E₂ (Cayman Chemical #14010). One or more of the following PDE inhibitors were also added at this time; 5 µM cilostamide (PDE3i) (Tocris #0915), 10 µM rolipram (PDE4i) (Tocris #1349), 30µM BRL50481 (PDE7i) (Tocris #2237), 200 nM PF-04957325 (PDE8i) (Pfizer), 50 µM IBMX (non-selective PDE inhibitor for all cAMP-PDEs except PDE8) (Sigma), or 200 µM IBMX. Some cells were also treated with 200 nM ITI-078 (PDE1i) (Intracellular Therapeutics)[1]. The structure of this compound is shown as compound # 38 in this reference[1]. Treated cultures were incubated in 2 ml of media, in 2 ml microfuge tubes, at 37°C, 5% CO₂ for 20 minutes.

cAMP measurements

Jurkat cells (1×10^7) were treated as previously stated. Cells were briefly centrifuged and the supernate discarded. Cell pellets were snap frozen in LN2, and stored at -80°C until analysis. Cell pellets were lysed by adding 1ml of 1:99 mixture of 11.65 M HCL: 95% ethanol. Pellets were dispersed using a P1000 Eppendorf pipet tip, and vortexed. Lysate was

incubated at room temperature for 30 min. Following incubation, the extraction volume was transferred to a fresh microfuge tube, and dried in a speed vacuum. The cAMP was re-suspended in 150 µl of 0.1 M HCl, acetylated, and assayed using a cAMP ELISA kit according to manufacturer's recommendations (Cayman Biochemical).

Immunoblot analysis

Jurkat cells (1×10^7) were treated with PDE inhibitors as previously stated. Cells were briefly centrifuged and the supernate discarded. Cell pellets were snap frozen in LN2, and stored at -80°C until analysis. Cells were lysed with 200 µl of Laemmli 2% SDS buffer containing 1 mM dithiothreitol (DTT), and 3% glycerol, vortexed briefly, and immediately placed in a boiling water bath. Samples were incubated for 7 minutes, vortexed, and centrifuged briefly. Twenty µl was loaded onto 6 or 10% polyacrylamide Tris Glycine SDS (1.5 mm thickness) gels. Electrophoresis was run at 150 V for 1 hour. Proteins were transferred to nitrocellulose at 34V for 16 hours. Immunoreactive bands were visualized and quantified using an Odyssey CLx imaging system using the 600 nm and 800 nm laser intensities set at 4 and 6 respectively. Membranes were blocked with PBS based Odyssey blocking buffer and then probed with primary antibodies in ½ diluted Odyssey blocking buffer containing 0.1% Tween20. Secondary antibodies (Licor) 1:25,000 in ½ diluted Odyssey blocking buffer, containing 0.1% Tween20, and 0.05 % SDS. All incubations were 1 hour. Membranes were washed with PBS, 0.1% Tween20, for 5 minutes each wash, for a total of 3 washes. A final wash before visualization was in PBS. Image Studio Light v5.2 was used to quantify scans, and Graphpad Prism was used to graph results.

Mass Spectrometry sample preparation

A label-free mass spectrometry approach was used for these studies[2]. Each biological condition was repeated a minimum of 3 times and at least a total of 3 analytical replicates each (minimum of 9 LC-MS/MS runs per condition) (Refer to Supplemental Figure 2 for experimental summary, and supplemental materials for details). After a 20-minute incubation with the indicated PDE inhibitors, adenylyl cyclase agonist, and CD3/CD28 antibodies, cells were centrifuged for 30 seconds at 20K x g. The supernate was aspirated and 250 µl of boiling lysis buffer was added: 6M guanidinium hydrochloride, 100 µl Tris-HCl pH 8.0, 5 mM Tris (2-carboxyethyl) phosphine (TCEP), and 10 mM chloroactamide (CAM). Tubes were vortexed briefly, and placed in a boiling water bath for 10 minutes. Tubes were again vortexed briefly, and then centrifuged at 20K x g for 30 seconds. Three µl of lysate was used for BCA protein quantification using a BSA standard, according to manufacturer's specifications (Pierce). One mg of lysate protein was transferred to a 1.5 ml, low binding microfuge tube (Axygen, MCT-200-L-C). An equal volume of 25 mM Tris pH 8.0 and 1:200 Lys-C (wt/wt) was added. Lysates were incubated at 37°C, with 200 rpm shaking for 2 hours. After 2 hours, 1 ml of 25 mM Tris pH 8.0, and 1:100 (wt/wt) of 1mg/ml Trypsin (in 50 mM acetic acid) was added. Lysates were incubated overnight, for a minimum of 16 hours, at 37°C with 200 rpm shaking. Digests were then acidified with 1% Trifluoroacetic acid (TFA), and centrifuged at 20K x g for 5 minutes. Supernates were applied to Waters Oasis 10mg extraction cartridges that were activated with reagents in the following order: 1 ml MeOH; 1 ml 80% Acetonitrile (ACN), 0.1% trifluoroacetic acid (TFA); then 1 ml 5% ACN, 0.1% TFA. Supernates were passed through the cartridges via vacuum, and syringe plunger to prevent resin from drying. Cartridges were washed three times with 1 ml 5% ACN, 0.1% TFA. Peptides were eluted from cartridges with 500 µl

80% ACN, 0.1% TFA into a 1.7 ml low binding microfuge tube. Elution was repeated for a total of three times, and then the eluates combined and dried in a speed vacuum, at ambient temperatures.

For enrichment of phosphopeptides, dried peptides were re-suspended in 300 µl of 80% ACN, 0.1% TFA. Reconstituted peptides were transferred to 1.5 ml low binding microfuge tube with 20 µl of IMAC slurry, a 1:1:1 slurry of Fe-NTA, Ga-NTA, and PHO-Select Fe-NTA (Sigma). Peptides were incubated at 25°C for 1 hour with 1500 rpm shaking. Post incubation, tubes were centrifuged briefly, and the IMAC resin was washed with 500 µl of 80% ACN, 0.1% TFA. Washes were repeated for a total of two washes. IMAC resin was applied to C18 StageTips[3] (two punches of C18 membrane, Empore C18 #2315) and the volume was passed through with a syringe. The C18 was washed twice with 150 µl, of 1% formic acid. Phosphopeptides were eluted twice from the IMAC resin with 150 µl of 500 mM K₂PO₄. C18 resin was washed twice with 150 µl of 1% formic acid. StageTips were stored at 4°C.

LC-MS/MS and data analysis

Peptides were eluted from StageTips with 50 µl of 80% ACN, 0.1% TFA, into a 96 well, conical bottom, polypropylene plate. Phosphopeptides were dried in a speed vacuum and resuspended in 12 µl of 5% ACN, 0.1% TFA. Three µl of phosphopeptides were applied to a self-pulled, 360 µm OD x 100 µm ID 20 cm column (with a 7 µm tip) packed with 3 µm diameter Reprosil C18 resin (Dr. Maisch GmbH, Germany). Peptides were analyzed in a 120 min, 5% to 30% acetonitrile gradient in 0.1% acetic acid at 300 nL/min on a nanoLC-MS (Thermo Dionex RSLCnano) and injected into an Orbitrap Elite. Orbitrap FTMS spectra (R = 30 000 at 400 m/z; m/z 350–1600; 3e6 target; max 500 ms ion injection time) and Top15 data dependent CID MS/MS spectra (1e4 target; max

100 ms injection time) were collected with dynamic exclusion for 30 s and an exclusion list size of 50. The normalized collision energy applied for CID was 35% for 10 ms. Mass spectra were searched against the Uniprot human reference proteome downloaded on July 29, 2015 and quantified using MaxQuant v1.5.2.8[4]. Under group-specific parameters, all default parameters were retained. Under global parameters, match between runs were selected: match time window and alignment time window were set to 0.7 and 20 respectively. Data analysis was performed using the Perseus[5] software suite.

Kinase Prediction

The web based NetPhorest program identifies probable kinases likely to phosphorylate queried sequences, based on the substrate consensus sequence motifs of 179 kinases. A truncated peptide sequence of 4 amino acid residues flanking both sides of the regulated phosphosite was used as an input sequence in NetPhorest[6]. The predictive threshold was set at 0.21.

Functional Prediction

The Predict Functional Phosphosites (pfp) database evaluates whether a phosphorylation at a specified amino acid is likely to alter protein function by evaluating the evolutionary conservation, degree of disorder, presence of structural features, and kinase association of the amino acid sequence containing the modification site. The same truncated peptide sequence of 4 amino acid residues flanking the regulated phosphosite was used as an input sequence to query the database:pfp_database_release_1_2_update_1_20160126. Downloaded from <http://pfp.biosino.org/pfp/>[7]

STRING (Search Tool for the Retrieval of Interacting Genes) analysis

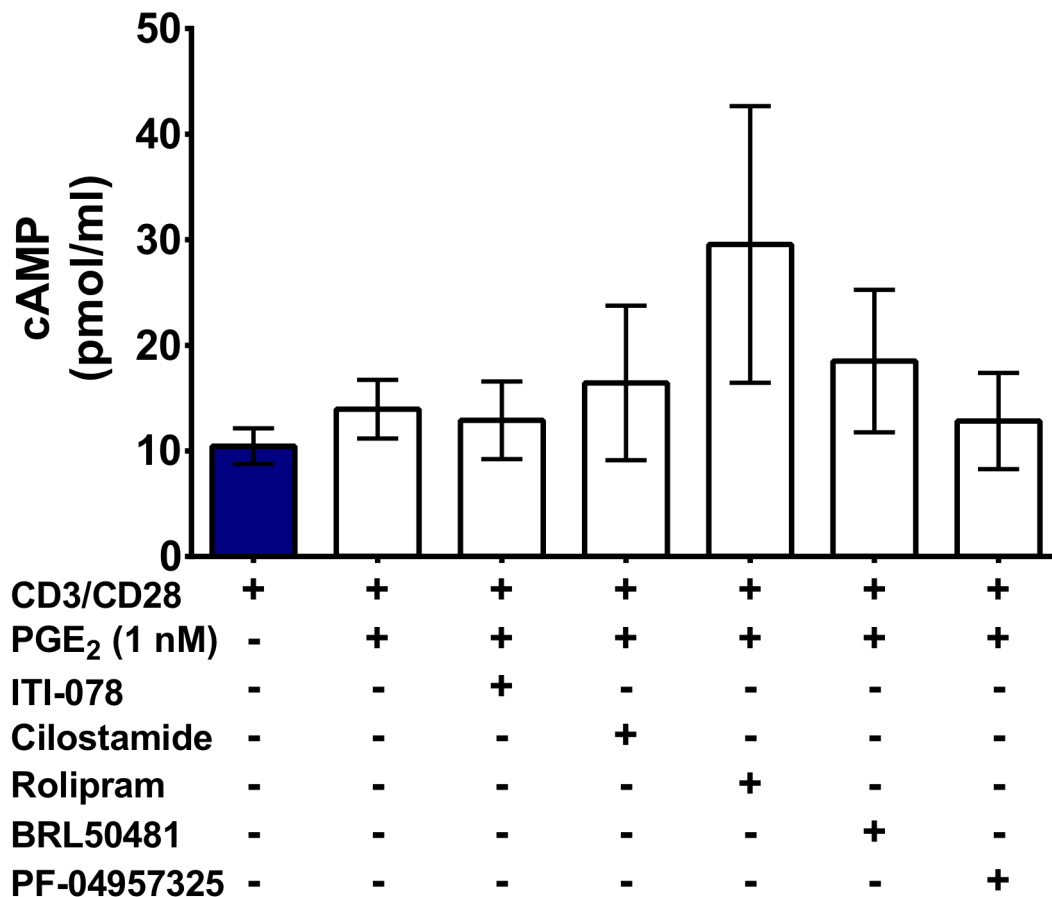
For each series of PDE inhibitor treatments, all statistically significant regulated phosphosites were compiled and lists of unique proteins were generated. Each protein list was used to query the STRING interaction database[8] (<http://string-db.org/>). “Experiments” and “Databases” source options were selected, and the minimum interaction score was set to 0.700. For visual clarity, disconnected nodes were omitted from the interaction map.

Gene ontology analysis

Gene ontology (GO) analysis was performed using the ClueGo Cytoscape plug in[9]. Lists of unique proteins, for each series of PDE inhibitor treatments, were generated from the statistically significant regulated phosphosites. Each list was used to query Kegg, Gene Ontology—biological function database, and Wikipathways. ClueGo parameters were set as indicated: Go Term Fusion selected; only display pathways with p values ≤ 0.05 ; GO tree interval, all levels; GO term minimum # genes, 3; threshold of 4% of genes per pathway; and a kappa score of 0.42. Gene ontology terms are presented as nodes and clustered together based on the similarity of genes present in each term or pathway. Node size is proportional to the P value for GO term enrichment, i.e. a larger node is generated from a smaller P value. Proteins are presented as smaller circles. Multicolored circles indicate proteins associated with more than one process.

Supplemental Figure 1

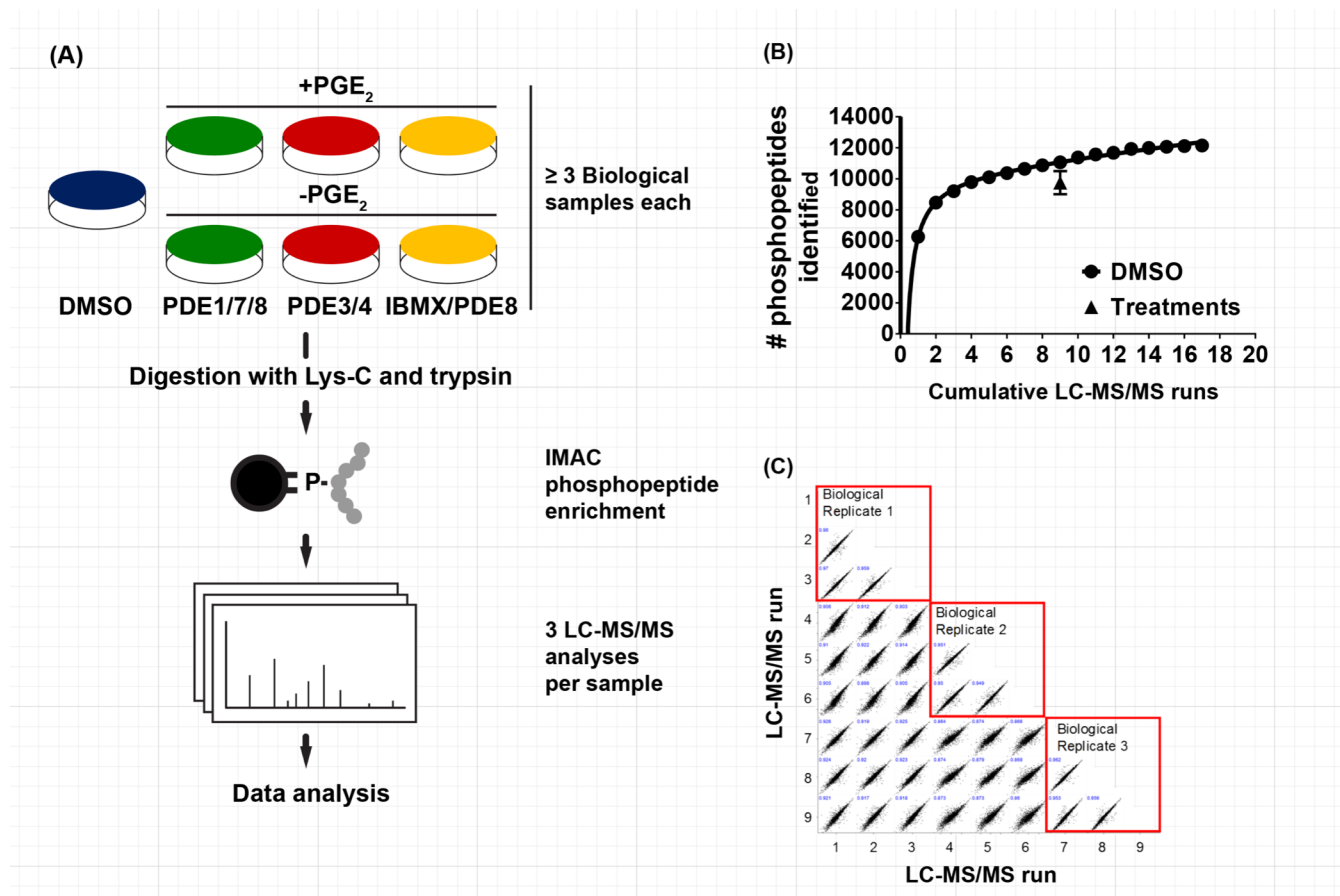
Effects of individual PDE inhibitors on cAMP in the presence of 1 nM PGE₂.



Cyclic AMP Measurements. 1×10^7 Jurkat cells were treated as indicated. Cells were briefly centrifuged and the supernate discarded. Cell pellets were lysed by adding 1ml of 1:99 mixture of 11.65 M HCL, and 95% EtOH. Pellets were dispersed using a P1000 pipet tip, and vortexed. Lysate was incubated at room temperature for 30 min. Following incubation, the extraction volume was transferred to a fresh microfuge tube, and dried in a speed vacuum. The cAMP was re-suspended in 150 μ l of 0.1 M HCl, acetylated, and assayed using a cAMP ELISA kit according to the manufacturer's recommendations (Cayman Biochemical). A two-tailed, t-test was performed to assess for statistically significant changes. No statistically significant changes in cAMP were observed. ITI-078 was used at 200 nM; cilostamide was used at 5 μ M; rolipram was used at 10 μ M, BRL50481 was used at 30 μ M; and PF-04957325 was used at 200 nM.

Supplemental Figure 2

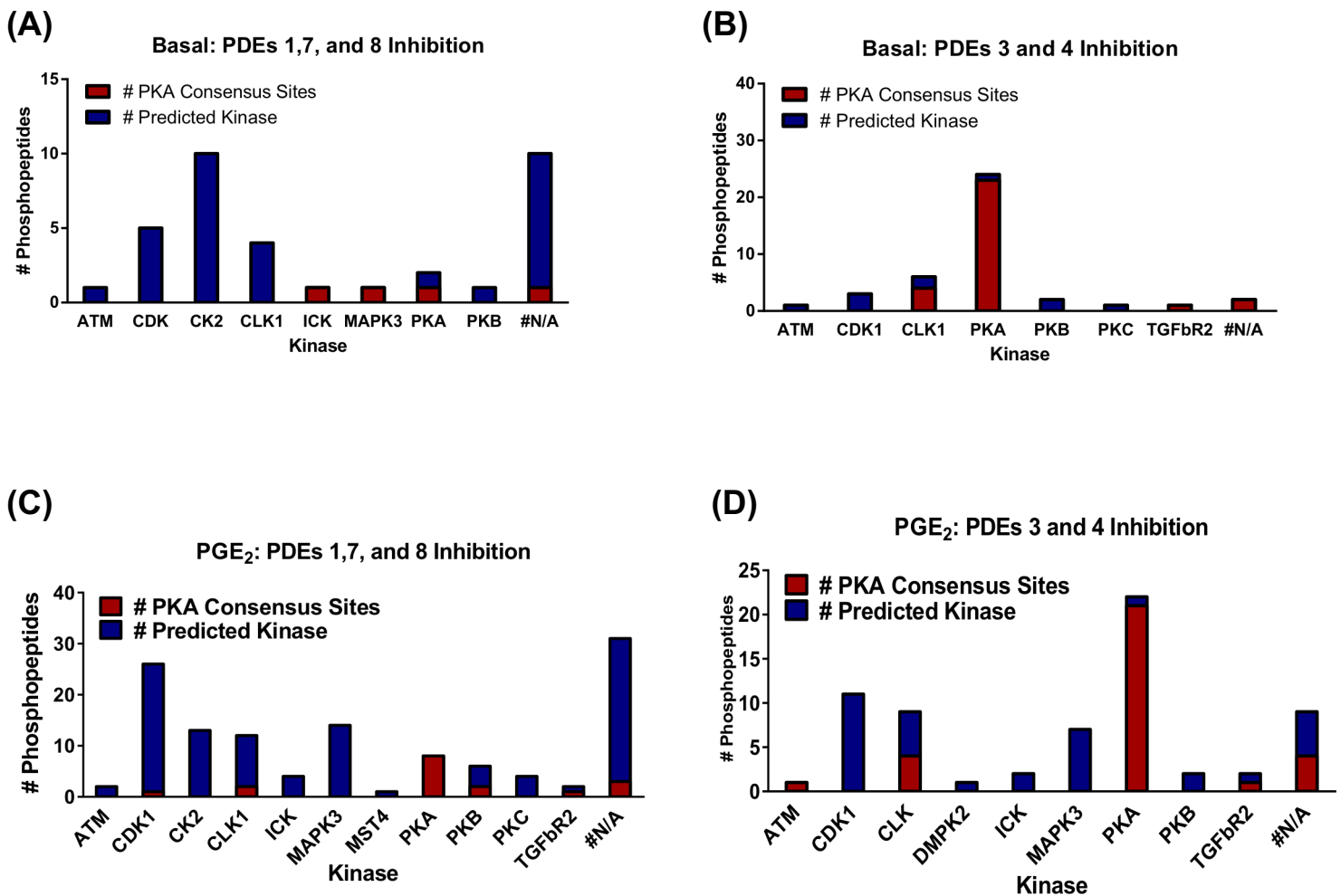
Outline of label-free mass spectrometry workflow and LC/MS/MS peptide identification efficiency.



Experimental Design (A) Jurkat (5×10^6) cells were cultured at 37°C , 5% CO_2 for one week in RPMI, 10% FBS, 2mM Glutamine, 100 U/ml Penicillin, and 100 $\mu\text{g}/\text{ml}$ Streptomycin. Twenty-four hours prior to experiment cells were washed and serum starved for 16 hours. After 16 hours, cells were synchronized by culturing in 50% FBS for 2 hours, followed by 1 hour of culture in serum free RPMI. Cells then were concurrently treated as indicated: 0.5 $\mu\text{g}/\text{ml}$ CD3, 0.5 $\mu\text{g}/\text{ml}$ CD28, 1 nM PGE_2 , 200 nM ITI-078, 5 μM cilostamide, 10 μM rolipram, 30 μM BRL50481, 200 nM PF-04957325, 50 μM IBMX, or 200 μM IBMX. Treated cultures were incubated at 37°C , 5% CO_2 for 20 minutes. (B) The total number of phosphopeptides identified in DMSO and PGE_2 conditions, with reported intensities, were counted and plotted as a function of the cumulative number of LC-MS/MS runs \bullet DMSO, \blacksquare PGE_2 (C). Scatter plots assessing the reproducibility of LC-MS/MS runs. The Pearson's correlation between phosphopeptide intensities between the PGE_2 IBMX/PF-04957325 LC-MS/MS runs are listed in blue. Red boxes highlight biological replicates, and analytical LC-MS/MS runs.

Supplemental Figure 3

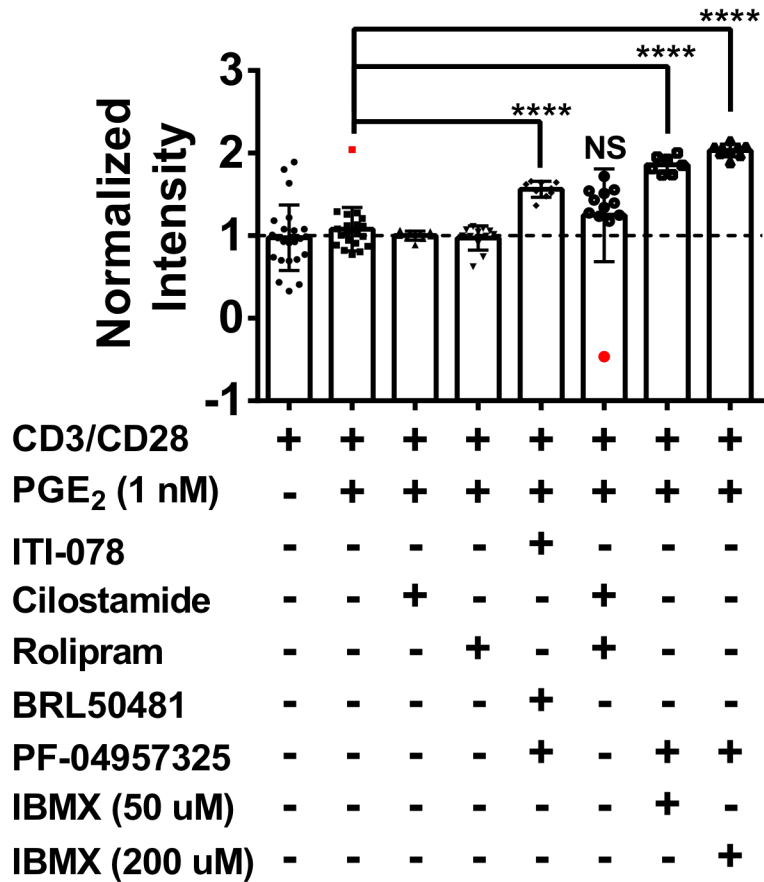
Distributions of the canonical PKA sequence compared to the predicted phosphorylating kinase.



Frequency of canonical PKA sequences that occur at sites predicted to be phosphorylated by PKA (or other kinases). A truncated peptide sequence of 4 amino acid residues flanking the regulated phosphosite was used as an input sequence in NetPhorest to predict kinases responsible for phosphorylating identified sites. Threshold score was set at 0.21. ATM= ataxi telangiectasia mutated kinase; CDK1 = Cyclin dependent kinase 1; CLK1 = CDC-like kinase; DMPK2 = Myotonic Dystrophy protein kinase-like protein (CDC42 binding protein kinase gamma); ICK = intestinal cell kinase; MAPK3 = mitogen activated protein kinase 3; MST4 = mammalian STE20-like protein kinase; PKA = cAMP-dependent protein kinase; PKB = protein kinase B (AKT), PKC = protein kinase C; TGFbR2 = transforming growth factor beta receptor 2; N/A = Not identified.

Supplemental Figure 6

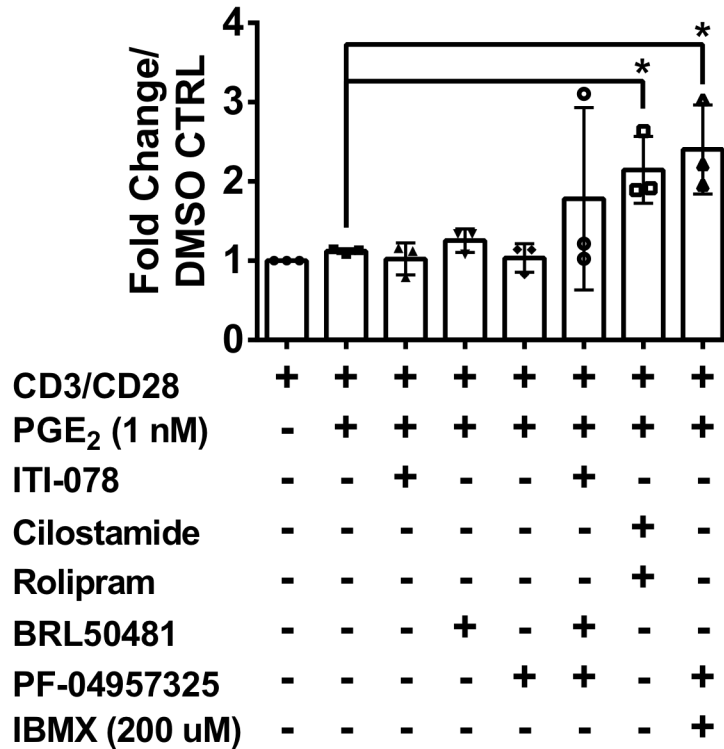
Fold increase in phosphorylation of ARHGEF2 S858 measured by mass spectrometry.



Analysis of ARHGEF2 mass spectrometry data. Values are normalized to the DMSO/CD3/CD28 control value (set to 1). Significant differences are seen only in the presence of prostaglandin plus the PDE8 inhibitor, the combination of PDE3+4 inhibitors, or the combination of IBMX and PDE8 inhibitor. No effect of the PDE1 inhibitor was noted either alone or in combination. Intensities from all LC/MS and all experimental conditions are plotted. Statistical outliers were identified in PRISM using the ROUT function, with a Q value of 1%. Outliers are highlighted in red.

Supplemental Figure 7

Comparison of changes in STMN1 S63 phosphorylation in response to two different combinations of PDE inhibitor treatment.



Immunoblot analysis of changes in Stathmin1 phosphorylation at S63. Jurkat (1×10^7) cells were treated as previously described. Cells were harvested and boiled in 200 μ l Laemmli buffer and transferred to nitrocellulose. Membranes were probed with anti-STMN1 antibody "S" 1:2000 (Abcam), and anti-Beta actin "B" 1:200,000 (Genetex). Membranes were quantified on the Odyssey Scanner Clx (Licor). Blot shown left, and quantified on the right. Statistical analysis was performed using a Student's t test. * $P \leq 0.02$,

Supplemental Table 1

List of genes comprising GO terms in functional cluster regulated by PDE1, 7, and 8 inhibition

Cluster	GO Term	Term P Value	Group P Value	Associated Genes Found
	alternative mRNA splicing, via spliceosome	21.0E-3	3.0E-3	[CDK13, DDX17, SFPQ , TRA2B]
	nucleotide-excision repair, DNA incision, 3'-to lesion	28.0E-3	3.5E-3	[BIVM-ERCC5, DDB2, ERCC5]
	Fas Ligand (FasL) pathway and Stress induction of Heat Shock Proteins (HSP) regulation	15.0E-3	2.1E-3	[ARHGDIB , LMNB1 , LMNB2, RB1]
	Regulation of Actin Cytoskeleton	1.1E-3	200.0E-6	[ARHGEF1, ARHGEF7 , BRAF , CFL1 , MAPK3 , PIK3C2A , SLC9A1 , SSH2]
	spindle organization	8.9E-3	1.4E-3	[ASUN, ATRX, CHD3 , CHMP2B , NCOR1 , SEPT1, TPR]
	regulation of fibroblast migration	49.0E-3	1.8E-3	[ARHGAP4, ARHGEF7 , BRAF]
	lamellipodium assembly	39.0E-3	3.4E-3	[ABLIM1, ARHGEF7 , HDAC4 , SSH2]
	DNA geometric change	3.9E-3	620.0E-6	[ATRX, CHD3 , DDB2, DDX3X, HNRNPA2B1, TP53BP1]
	positive regulation of viral process	46.0E-3	3.3E-3	[CFL1 , CHMP2B , DDX3X, POLR2A, YTHDC2]
	ATM Signaling Network in Development and Disease	17.0E-3	3.7E-3	[HDAC4 , MDC1, RIF1, TP53BP1]
	double-strand break repair via nonhomologous end joining	47.0E-3	3.7E-3	[MDC1, RIF1, TFIP11, TP53BP1]
	T cell selection	16.0E-3	1.4E-3	[BCL11B , BRAF , FASN, ITPKB]
	alpha-beta T cell differentiation	23.0E-3	1.4E-3	[BCL11B , BRAF , ITPKB, SASH3, SATB1]
	gene silencing by RNA	5.1E-3	580.0E-6	[EIF4G1, HNRNPA2B1, NCOR1 , NUP50 , POLR2A, SNIP1, TPR]
	negative regulation of translation	8.9E-3	580.0E-6	[DDX3X, EIF2AK2 , EIF4G1, HNRNPA2B1, NCOR1 , SNIP1, TPR]
	gene silencing by miRNA	36.0E-3	580.0E-6	[EIF4G1, HNRNPA2B1, NCOR1 , SNIP1]

Supplemental Table 1. List of genes comprising GO terms in functional clusters regulated by combined PDE1, 7, and 8 inhibitors. Gene ontology (GO) analysis was performed using the ClueGo Cytoscape plug in. Lists of unique proteins for PDEs 1, 7, and 8 inhibitor treatment were generated from the statistically significant regulated phosphosites. Each list was used to query KEGG, Gene Ontology—biological function database, and Wikipathways. ClueGo parameters were set as indicated: Go Term Fusion selected; only display pathways with p values ≤ 0.05 ; GO tree interval, all levels; GO term minimum # genes, 3; threshold of 4% of genes per pathway; and kappa score of 0.42. **Bolded genes** have regulated phosphosites predicted to be functional. In addition, **Red bolded genes** are sites with a PKA consensus site.

Supplemental Table 1 (continued)

List of genes comprising GO terms in functional cluster regulated by PDE1, 7, and 8 inhibition

Cluster	GO Term	Term P Value	Group P Value	Associated Genes Found
	Thyroid cancer	41.0E-3	62.0E-6	[BRAF , MAPK3 , TPR]
	regulation of chromosome segregation	3.2E-3	62.0E-6	[ATRX, DYNC1L1, MKI67, RB1 , SFPQ , TPR]
	regulation of chromatin organization	14.0E-3	62.0E-6	[ATRX, MAPK3 , MKI67, RIF1, RTF1 , TP53BP1 , TPR]
	regulation of sister chromatid cohesion	21.0E-3	62.0E-6	[ATRX, RB1 , SFPQ]
	positive regulation of chromatin organization	31.0E-3	62.0E-6	[MAPK3 , RIF1, RTF1 , TP53BP1 , TPR]
	positive regulation of chromosome organization	280.0E-6	62.0E-6	[ATRX, HNRNPA2B1, MAPK3 , RB1 , RIF1, RTF1 , SFPQ , TP53BP1 , TPR]
	mRNA Processing	3.8E-3	11.0E-9	[CLASRP , HNRNPA2B1, POLR2A, SFPQ , SRRM1, SUGP2, TRA2B]
	mRNA processing	6.7E-9	11.0E-9	[BUD13, CDK13, CLASRP , DDX17, FIP1L1, HNRNPA2B1, LIN9, PNN, POLR2A, SAFB, SAFB2, SFPQ , SPEN, SRRM1, SRRM2, SUGP2, TFIP11, TRA2A, TRA2B, WDR33 , YTHDC1]
	RNA splicing	34.0E-9	11.0E-9	[BUD13, CDK13, CLASRP , DDX17, FIP1L1, HNRNPA2B1, LIN9, PNN, POLR2A, SFPQ , SPEN, SRRM1, SRRM2, SUGP2, TFIP11, TRA2A, TRA2B, WDR33 , YTHDC1]
	regulation of RNA splicing	45.0E-3	11.0E-9	[DDX17, HNRNPA2B1, POLR2A, TRA2B, YTHDC1]
	regulation of mRNA processing	7.3E-3	11.0E-9	[DDX17, HNRNPA2B1, SAFB, SAFB2, TRA2B, YTHDC1]
	mRNA splicing, via spliceosome	20.0E-9	11.0E-9	[BUD13, CDK13, DDX17, FIP1L1, HNRNPA2B1, LIN9, PNN, POLR2A, SFPQ , SPEN, SRRM1, SRRM2, TFIP11, TRA2A, TRA2B, WDR33 , YTHDC1]

Supplemental Table 1 (continued). List of genes comprising GO terms in functional cluster regulated by combined PDE1, 7, and 8 inhibitors. Gene ontology (GO) analysis was performed using the ClueGo Cytoscape plug in. Lists of unique proteins for PDEs 1, 7, and 8 inhibitor treatment were generated from the statistically significant regulated phosphosites. Each list was used to query KEGG, Gene Ontology—biological function database, and Wikipathways. ClueGo parameters were set as indicated: Go Term Fusion selected; only display pathways with p values ≤ 0.05 ; GO tree interval, all levels; GO term minimum # genes, 3; threshold of 4% of genes per pathway; and kappa score of 0.42. **Bolded genes** have regulated phosphosites predicted to be functional. In addition, **Red bolded genes** are sites with a PKA consensus site.

Supplemental Table 1 (continued)

List of genes comprising GO terms in functional cluster regulated by PDE1, 7, and 8 inhibition

Cluster	GO Term	Term P Value	Group P Value	Associated Genes Found
	RNA transport	14.0E-3	2.4E-6	[<i>EIF2S2</i> , EIF4G1, <i>NUP50</i> , PNN, SRRM1, TPR, <i>XPO1</i>]
	ribonucleoprotein complex localization	46.0E-6	2.4E-6	[BUD13, FIP1L1, HNRNPA2B1, LIN9, <i>NUP50</i> , SRRM1, TPR, <i>WDR33</i> , <i>XPO1</i>]
	RNA transport	25.0E-6	2.4E-6	[ATXN2, BICD2, BUD13, FIP1L1, HNRNPA2B1, LIN9, <i>NUP50</i> , SRRM1, TPR, <i>WDR33</i> , <i>XPO1</i>]
	intracellular transport of virus	16.0E-3	2.4E-6	[<i>NUP50</i> , TPR, <i>XPO1</i>]
	mRNA transport	210.0E-6	2.4E-6	[BICD2, BUD13, FIP1L1, HNRNPA2B1, <i>NUP50</i> , SRRM1, TPR, <i>WDR33</i> , <i>XPO1</i>]
	protein export from nucleus	690.0E-6	2.4E-6	[BUD13, FIP1L1, HNRNPA2B1, <i>NUP50</i> , SRRM1, <i>TP53BP1</i> , TPR, <i>WDR33</i> , <i>XPO1</i>]
	regulation of chromosome segregation	3.2E-3	120.0E-9	[ATRX, DYNC1LI1, MKI67, <i>RB1</i> , <i>SFPQ</i> , TPR]
	sister chromatid segregation	640.0E-6	120.0E-9	[ATRX, CHAMP1, <i>CHMP2B</i> , DYNC1LI1, KIF22, <i>RB1</i> , <i>SFPQ</i> , STAG2, TPR, <i>XPO1</i>]
	metaphase plate congression	27.0E-3	120.0E-9	[CHAMP1, <i>CHMP2B</i> , KIF22, SEPT1]
	sister chromatid cohesion	19.0E-3	120.0E-9	[ATRX, KIF22, <i>RB1</i> , <i>SFPQ</i> , STAG2, <i>XPO1</i>]
	mitotic sister chromatid segregation	6.0E-3	120.0E-9	[ATRX, CHAMP1, <i>CHMP2B</i> , DYNC1LI1, KIF22, <i>RB1</i> , TPR]
	regulation of mitotic nuclear division	9.5E-3	120.0E-9	[ATRX, CDK13, <i>CHMP2B</i> , DYNC1LI1, MKI67, <i>RB1</i> , TPR]
	regulation of sister chromatid cohesion	21.0E-3	120.0E-9	[ATRX, <i>RB1</i> , <i>SFPQ</i>]
	positive regulation of chromosome organization	280.0E-6	120.0E-9	[ATRX, HNRNPA2B1, <i>MAPK3</i> , <i>RB1</i> , RIF1, <i>RTF1</i> , <i>SFPQ</i> , <i>TP53BP1</i> , TPR]

Supplemental Table 1 (continued). List of genes comprising GO terms in functional cluster regulated by combined PDE1, 7, and 8 inhibitors. Gene ontology (GO) analysis was performed using the ClueGo Cytoscape plug in. Lists of unique proteins for PDEs 1, 7, and 8 inhibitor treatment were generated from the statistically significant regulated phosphosites. Each list was used to query KEGG, Gene Ontology—biological function database, and Wikipathways. ClueGo parameters were set as indicated: Go Term Fusion selected; only display pathways with p values ≤ 0.05 ; GO tree interval, all levels; GO term minimum # genes, 3; threshold of 4% of genes per pathway; and kappa score of 0.42. **Bolded genes** have regulated phosphosites predicted to be functional. In addition, **Red bolded genes** are sites with a PKA consensus site.

Supplemental Table 1 (continued)

List of genes comprising GO terms in functional cluster regulated by PDE1, 7, and 8 inhibition

Cluster	GO Term	Term P Value	Group P Value	Associated Genes Found
	Dorso-ventral axis formation	39.0E-3	860.0E-12	[BRAF , ETS1 , MAPK3]
	B cell receptor signaling pathway	16.0E-3	860.0E-12	[MAPK3 , NFATC3 , PRKCB]
	Fc gamma R-mediated phagocytosis	26.0E-3	860.0E-12	[CFL1 , CRKL, MAPK3 , MARCKSL1 , PRKCB]
	Long-term potentiation	40.0E-3	860.0E-12	[BRAF , MAPK3 , PRKCB]
	Thyroid hormone signaling pathway	12.0E-3	860.0E-12	[MAPK3 , NCOR1 , PRKCB , SLC9A1 , STAT1 , TBC1D4]
	Hepatitis B	6.4E-3	860.0E-12	[DDB2, DDX3X, MAPK3 , NFATC3 , PRKCB , RB1 , STAT1]
	Renal cell carcinoma	46.0E-3	860.0E-12	[BRAF , CRKL, ETS1 , MAPK3]
	Pancreatic cancer	45.0E-3	860.0E-12	[BRAF , MAPK3 , RB1 , STAT1]
	Glioma	45.0E-3	860.0E-12	[BRAF , MAPK3 , PRKCB , RB1]
	Thyroid cancer	41.0E-3	860.0E-12	[BRAF , MAPK3 , TPR]
	Melanoma	31.0E-3	860.0E-12	[BRAF , MAPK3 , RB1]
	Chronic myeloid leukemia	11.0E-3	860.0E-12	[BRAF , CRKL, MAPK3 , RB1 , RUNX1]
	Non-small cell lung cancer	3.7E-3	860.0E-12	[BRAF , MAPK3 , PRKCB , RB1 , STK4]
	Human Thyroid Stimulating Hormone (TSH) signaling pathway	8.6E-3	860.0E-12	[BRAF , MAPK3 , RAP1GAP, RB1 , STAT1]
	Signaling Pathways in Glioblastoma	17.0E-3	860.0E-12	[BRAF , MAPK3 , PIK3C2A , PRKCB , RB1]
	B Cell Receptor Signaling Pathway	30.0E-3	860.0E-12	[BRAF , CRKL, ETS1 , NFATC3 , PRKCB]
	Kit receptor signaling pathway	36.0E-3	860.0E-12	[CRKL, MAPK3 , PRKCB , STAT1]
	EGF/EGFR Signaling Pathway	11.0E-3	860.0E-12	[ARHGEF1, ATXN2, BRAF , CFL1 , CRKL, PRKCB , STAT1]
	epithelial cell apoptotic process	31.0E-3	860.0E-12	[BRAF , FASN, HIPK1, RB1 , STK4]
	positive regulation of chromatin organization	31.0E-3	860.0E-12	[MAPK3 , RIF1, RTF1 , TP53BP1 , TPR]
	hepatocyte apoptotic process	11.0E-3	860.0E-12	[FASN, RB1 , STK4]

Supplemental Table 1 (continued). List of genes comprising GO terms in functional cluster regulated by PDE1, 7, and 8 inhibition. Gene ontology (GO) analysis was performed using the ClueGo Cytoscape plug in. Lists of unique proteins for PDEs 1, 7, and 8 inhibitor treatment were generated from the statistically significant regulated phosphosites. Each list was used to query KEGG, Gene Ontology—biological function database, and Wikipathways. ClueGo parameters were set as indicated: Go Term Fusion selected; only display pathways with p values ≤ 0.05 ; GO tree interval, all levels; GO term minimum # genes, 3; threshold of 4% of genes per pathway; and kappa score of 0.42. **Bolded genes** have regulated phosphosites predicted to be functional. In addition, **Red bolded genes** are sites with a PKA consensus site.

Supplemental Table 2

List of genes comprising GO terms in functional cluster regulated by PDE3, and 4 inhibition

Cluster	GO Term	Term P Value	Group P Value	Associated Genes Found
	double-strand break repair via nonhomologous end joining	5.3E-3	2.6E-3	[MDC1 , RIF1 , SMC5]
	Pathways Affected in Adenoid Cystic Carcinoma	7.3E-3	4.9E-3	[ARID1A, HIST1H1E, MAP2K2]
	establishment of spindle orientation	1.1E-3	490.0E-6	[ARHGEF2, MAP4, NUMA1]
	Chronic myeloid leukemia	3.2E-3	2.8E-3	[ABL1 , BAD , MAP2K2]
	Amyotrophic lateral sclerosis (ALS)	2.9E-3	2.8E-3	[ALS2, BAD , MAP2K2]
	histone H3-K27 trimethylation	98.0E-6	53.0E-6	[HIST1H1C, HIST1H1D, HIST1H1E]
	peptidyl-lysine trimethylation	200.0E-6	53.0E-6	[HIST1H1C, HIST1H1D, HIST1H1E, PWP1]
	histone lysine methylation	100.0E-6	53.0E-6	[HIST1H1C, HIST1H1D, HIST1H1E, PWP1, RIF1 , SNW1]
	histone H3-K4 methylation	730.0E-6	53.0E-6	[HIST1H1C, HIST1H1D, HIST1H1E, SNW1]
	Regulation of Microtubule Cytoskeleton	4.1E-3	270.0E-6	[ABL1 , CLIP1, STMN1]
	regulation of microtubule cytoskeleton organization	200.0E-6	270.0E-6	[ABL1 , ARHGEF2, CLIP1, GAS2L1, RANBP2, STMN1]
	negative regulation of microtubule polymerization or depolymerization	1.6E-3	270.0E-6	[ARHGEF2, GAS2L1, STMN1]
	regulation of microtubule polymerization	1.7E-3	270.0E-6	[ABL1 , CLIP1, STMN1]
	protein depolymerization	3.5E-3	270.0E-6	[ARHGEF2, GAS2L1, MICAL1, STMN1]

Legend -- List of genes comprising GO terms in functional cluster regulated by PDE3, and 4 inhibition. Gene ontology (GO) analysis was performed using the ClueGo Cytoscape plug in. Lists of unique proteins for PDEs 3 and 4inhibitor treatment were generated from the statistically significant regulated phosphosites. Each list was used to query KEGG, Gene Ontology—biological function database, and Wikipathways. ClueGo parameters were set as indicated: Go Term Fusion selected; only display pathways with p values ≤ 0.05 ; GO tree interval, all levels; GO term minimum # genes, 3; threshold of 4% of genes per pathway; and kappa score of 0.42. **Bolded genes** have regulated phosphosites predicted to be functional. In addition, **Red bolded genes** are sites with a PKA consensus site.

Expanded discussion of PDE-modulated functional compartments.

STRING analysis of the PDE 1,7, and 8 inhibitor phosphosites, suggests a cAMP mediated regulatory action on the phosphatase, PTPN7, a known regulator of MAPK3 and other kinases in this cascade. There are 15 phosphosites modulated under the PDE 1, 7, and 8 inhibitor condition that are predicted to be phosphorylated by MAPK3. Likely examples of indirect cAMP signaling via phosphatase regulation include: BAP18 S76, CHAMP1 S286, CHD3 S1660, CHD3 S1660, ITPKB S43, LIN9 S380, LMNB1 S391, NCOR1 S2048, PIK33C2A 1553, RB1 T778, RING1 S254, SMEK1 S728, SNIP1 S54, SNTB2 S393, AND STAT1 S727.

Interestingly, Conche et al.[10] previously implicated PTPN7, ERK, and a cAMP mediated signal as an early enhancer of the T cell receptor response promoted by cellular adhesion. We found that phosphosites on ARHGEF2, BRAF, LASP1 and PTPN7 were regulated by inhibiting PDEs 1, 7, and 8; whereas sites on CAD, BAD, CAMKK1, PTPN7, and STMN1 were regulated by inhibiting PDEs 3 and 4. ARHGEF2[11], BRAF[12], and LASP1[13] have been associated with regulation of cytoskeletal organization and cell adhesion/migration. It is plausible that inhibiting a combination of PDEs 1, 7, and 8 could therefore regulate T cell migration and activation. Since PDE1 protein and activity is reported to be low in several T cell models, this perhaps suggests that the most important combination will be PDE7 and PDE8 inhibitors.

PDE 3 and 4 inhibition also significantly increased the phosphorylation of CAD (Table 2), the rate limiting protein in the pyrimidine biosynthetic pathway. Increased glutamine metabolism in lymphocytes is thought to be required to support proliferation, and provide metabolites for biosynthetic pathways[14-16]. CAD is a multi-domain protein that catalyzes the

first reactions of de novo pyrimidine biosynthesis, converting glutamine to carbamoyl phosphate. UTP binding to the BH3 regulatory domain of CAD, causes feedback inhibition. Phosphorylation of S1406 prevents UTP binding and increases activity of the enzyme[17]. Paradoxically, it seems that phosphorylation of S1406 on CAD would increase glutamine metabolism and promote T cell activation. However, the combination treatment of PDEs 3 and 4 inhibitor has been shown to inhibit T cell function. One possible explanation is that an overactive pyrimidine biosynthetic pathway reduces the available glutamine that can be converted to glutamate and shuttled into the TCA cycle or converted to glutathione. This should reduce the cells ability to buffer against reactive oxygen species generated by rapid proliferation, and could be a novel mechanism of cAMP-dependent inhibition of T cell function.

Similarly, S163 of DGKZ is one of the most consistently phosphorylated sites in the PDE3 plus PDE4 inhibitor condition. A number of T cell functions are known to be controlled by DGKZ[18]. For example, it is well established that redistribution of diacylglycerol kinase to the immunological synapse can regulate several aspects of T cell activation[19] and function including T cell adhesion and migration[20]. Activation of DGKZ would be expected to lower diacylglycerol and increase phosphatidic acid, both of which are likely to decrease T cell activation. Much less is known about a possible role for cAMP-dependent phosphorylation of S163 as a regulator of T cells though one would predict that activation of the enzyme would be consistent with an inhibitory effect of PDE 3 plus 4 inhibition on T cell activation. Further studies will be needed to test how much of the inhibitory effect of cAMP on T cell function might be localized to this phosphosite and regulated by a combination of both PDE3 and PDE4.

References - Supplemental

1. Li, P., et al., *Discovery of Potent and Selective Inhibitors of Phosphodiesterase 1 for the Treatment of Cognitive Impairment Associated with Neurodegenerative and Neuropsychiatric Diseases*. J Med Chem, 2016. **59**(3): p. 1149-64.
2. Jersie-Christensen, R.R., A. Sultan, and J.V. Olsen, *Simple and Reproducible Sample Preparation for Single-Shot Phosphoproteomics with High Sensitivity*. Methods Mol Biol, 2016. **1355**: p. 251-60.
3. Rappsilber, J., Y. Ishihama, and M. Mann, *Stop and go extraction tips for matrix-assisted laser desorption/ionization, nanoelectrospray, and LC/MS sample pretreatment in proteomics*. Anal Chem, 2003. **75**(3): p. 663-70.
4. Cox, J. and M. Mann, *MaxQuant enables high peptide identification rates, individualized p.p.b.-range mass accuracies and proteome-wide protein quantification*. Nat Biotechnol, 2008. **26**(12): p. 1367-72.
5. Tyanova, S., et al., *The Perseus computational platform for comprehensive analysis of (prote)omics data*. Nat Methods, 2016. **13**(9): p. 731-40.
6. Horn, H., et al., *KinomeXplorer: an integrated platform for kinome biology studies*. Nat Methods, 2014. **11**(6): p. 603-4.
7. Xiao, Q., et al., *Prioritizing functional phosphorylation sites based on multiple feature integration*. Sci Rep, 2016. **6**: p. 24735.
8. Szklarczyk, D., et al., *STRING v10: protein-protein interaction networks, integrated over the tree of life*. Nucleic Acids Res, 2015. **43**(Database issue): p. D447-52.
9. Bindea, G., et al., *ClueGO: a Cytoscape plug-in to decipher functionally grouped gene ontology and pathway annotation networks*. Bioinformatics, 2009. **25**(8): p. 1091-3.
10. Conche, C., et al., *T cell adhesion primes antigen receptor-induced calcium responses through a transient rise in adenosine 3',5'-cyclic monophosphate*. Immunity, 2009. **30**(1): p. 33-43.
11. Meiri, D., et al., *Mechanistic insight into the microtubule and actin cytoskeleton coupling through dynein-dependent RhoGEF inhibition*. Mol Cell, 2012. **45**(5): p. 642-55.
12. Brown, W.S., et al., *B-Raf regulation of integrin alpha4beta1-mediated resistance to shear stress through changes in cell spreading and cytoskeletal association in T cells*. J Biol Chem, 2014. **289**(33): p. 23141-53.
13. Mihlan, S., et al., *Nuclear import of LASP-1 is regulated by phosphorylation and dynamic protein-protein interactions*. Oncogene, 2013. **32**(16): p. 2107-13.
14. Sugimoto, K., et al., *A clinically attainable dose of L-asparaginase targets glutamine addiction in lymphoid cell lines*. Cancer Sci, 2015. **106**(11): p. 1534-43.
15. Nakaya, M., et al., *Inflammatory T cell responses rely on amino acid transporter ASCT2 facilitation of glutamine uptake and mTORC1 kinase activation*. Immunity, 2014. **40**(5): p. 692-705.
16. Newsholme, E.A., B. Crabtree, and M.S. Ardawi, *Glutamine metabolism in lymphocytes: its biochemical, physiological and clinical importance*. Q J Exp Physiol, 1985. **70**(4): p. 473-89.
17. Kotsis, D.H., et al., *Protein kinase A phosphorylation of the multifunctional protein CAD antagonizes activation by the MAP kinase cascade*. Mol Cell Biochem, 2007. **301**(1-2): p. 69-81.
18. Krishna, S. and X. Zhong, *Role of diacylglycerol kinases in T cell development and function*. Crit Rev Immunol, 2013. **33**(2): p. 97-118.
19. Gharbi, S.I., et al., *Diacylglycerol kinase zeta controls diacylglycerol metabolism at the immunological synapse*. Mol Biol Cell, 2011. **22**(22): p. 4406-14.
20. Baldanzi, G., et al., *Diacylglycerol Kinases: Shaping Diacylglycerol and Phosphatidic Acid Gradients to Control Cell Polarity*. Front Cell Dev Biol, 2016. **4**: p. 140.